VIBRATION-FATIGUE ASSESSMENT ON ELECTRONICS INTERCONNECTIONS

By:

WONG ZIE JEN

(Matric no.: 142519)

Supervisor:

Assoc. Prof. Dr. Abdullah Aziz Bin Saad

July 2022

This dissertation is submitted to
Universiti Sains Malaysia
As partial fulfillment of the requirement to graduate with honors degree in
BACHELOR OF ENGINEERING (MECHANICAL ENGINEERING)

School of Mechanical Engineering
Engineering Campus
Universiti Sains Malaysia

DECLARATION

This work has not been accepted in substance for any degree and is not being concurrently submitted in candidature for any degree.

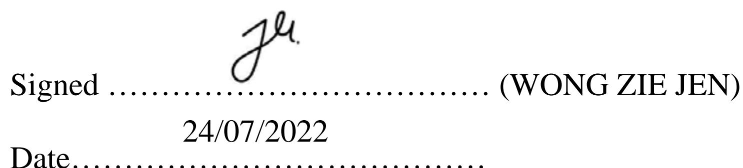

Signed ……………………………… (WONG ZIE JEN)

Date………………………………… 24/07/2022

Statement 1: This journal is the result of my own investigation, except where otherwise stated. Other sources are acknowledged by giving explicit references. Bibliography/references are appended.

Signed……………………………… (WONG ZIE JEN)

Date………………………………… 24/07/2022

Statement 2: I hereby give consent for my journal, if accepted, to be available for photocopying and for interlibrary loan, and for the title and summary to be made available outside organizations.

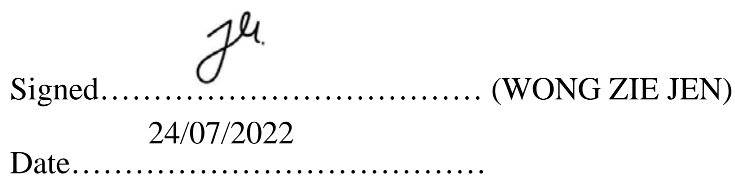

Signed……………………………… (WONG ZIE JEN)

Date………………………………… 24/07/2022

ACKNOWLEDGEMENT

First and foremost, I would like to give my utmost gratitude to the School of Mechanical Engineering, Universiti Sains Malaysia for providing the required equipment and the necessary materials to complete my Final Year Project (FYP). Besides, I would like to express my gratitude to my supervisor, Assoc. Prof. Dr. Abdullah Aziz Saad for continuous support and guidance throughout the whole project. I am very thankful of the time allocated for meeting me. I am grateful of the help and ideas given as I am finishing this project. Furthermore, I would also like to acknowledge with much appreciation the crucial role of the staffs of Vibration Lab of School of Mechanical Engineering, Universiti Sains Malaysia (USM), Mr. Wan Mohd. Amri bin Wan Mamat Ali who have provided insight and expertise that greatly assisted the research. Besides, many thanks go to the coordinator of this course, Dr. Muhammad Fauzinizam Bin Razali, who has invested his full effort in helping us achieve our goal. Last but not least, I have to appreciate my beloved family and friends for the moral support and encouragement which helped me in the completion of this research.

TABLE OF CONTENTS

DECLARATION ii

ACKNOWLEDGEMENT iii

TABLE OF CONTENTS iv

LIST OF FIGURES vii

LIST OF TABLES ix

LIST OF ABBREVIATIONS x

ABSTRAK xi

ABSTRACT xii

Chapter 1 INTRODUCTION 1

1.1 Overview of Project 1

1.2 Problem Statement 2

1.3 Objectives 3

1.4 Scope of Project 3

Chapter 2 LITERATURE REVIEW 4

2.1 Introduction 4

2.2 Overview of Electrically Conductive Adhesive 4

2.3 Fracture Behaviour of Electrically Conductive Adhesive 5

2.4 Random Vibration Test on Electronics Interconnection 7

2.5 Finite element analysis (FEA) 9

2.6 Fatigue life analysis 12

2.7 Critical evaluation 13

Chapter 3 RESEARCH METHODOLOGY 15

3.1 Introduction 15

3.2 FEA Geometry Modelling 15

3.3 Material Assignment 17

3.4 Meshing 19

3.5 Modal Analysis 20

3.6 Random Vibration Analysis 21

3.7 Harmonic Response Analysis 23

3.8 Vibration Fatigue Life Analysis 24

Chapter 4 RESULTS AND DISCUSSION 28

4.1 Overview 28

4.2 Mesh Independence Study 28

4.3 Modal Analysis 30

4.4 Random Vibration Analysis 32

4.4.1 Directional Deformation under Random Vibration Loading 32

4.4.2 Equivalent Stress under Random Vibration Loadings 35

4.4.3 Response Power Spectral Density (PSD) under Random Vibration Loading 42

4.5 Harmonic Response Analysis 45

4.6 Vibration Fatigue Life Analysis 47

Chapter 5 CONCLUSION AND FUTURE WORK 51

5.1 Overview ... 51

5.2 Conclusion ... 51

5.3 Recommendation For Future Works ... 52

REFERENCES ... 54

APPENDICES ... 62

APPENDIX A: Dimension of Geometry Model ... 62

APPENDIX B: Material Properties ... 65

APPENDIX C: JEDEC PSD Input ... 72

APPENDIX D: Steinberg Fatigue Limit Equation ... 73

LIST OF FIGURES

Figure 1-1. Cross sectional profile of the failed solder joints 1

Figure 2-1. Observed failure modes at the ECA joint 6

Figure 2-2. Cross sectional SEM images of fatigue tested specimens. (a) 298K (b) 398K 6

Figure 2-3. LED samples with solder joints 7

Figure 2-4. Vibration Test setup for LEDs joints 8

Figure 2-5. Random vibration test set up and measurement system............................ 8

Figure 2-6. FEA model of PCB assembly for modal analysis 9

Figure 2-7. 2D FEA model and boundary condition for the PQFP lead joint 9

Figure 2-8. The von Mises stress contour and critical areas for Cu lead and solder joint 10

Figure 2-9. The FEA mesh of the solder balls 10

Figure 2-10. The FEA model under a harmonic vibration excitation......................... 11

Figure 2-11. The configuration of (a) DC-DC converter and (b) MOSFET electronic package 11

Figure 2-12. Band range of frequency and the PSD amplitudes................................ 12

Figure 2-13. Plot of (a) stress, (b) accumulated strain, and (c) strain energy in the solder layer.. 12

Figure 3-1. The CAD model of solder 16

Figure 3-2. The CAD model of LED soldered on circuit pad.................................... 16

Figure 3-3. Complete assembly model 16

Figure 3-4. Close-up look of the mesh for LED soldered to circuit pad 19

Figure 3-5. Complete mesh of the FEA simulation model 20

Figure 3-6. Fixed support applied on the model for modal analysis.......................... 21

Figure 3-7. Fitted Power Spectral Density (PSD) input curve from 3 Hz to 2000 Hz 22

Figure 3-8. Component and Lead Wired undergoing Bending Motion 24

Figure 3-9. Circuit board fatigue analysis in Steinberg toolbox 26

Figure 3-10. SDOF Response to Base Input analysis 26

Figure 3-11. Steinberg Fatigue Damage toolbox 27

Figure 4-1. Mesh independence study for (i) Mesh 1 (ii) Mesh 2 (iii) Mesh 3 29

Figure 4-2. The number of vibration mode with significant deformation 31

Figure 4-3. Illustration of global directional deformation (3σ) in FEA model 34

Figure 4-4. Directional deformation (3σ) at solder joint.. 35

Figure 4-5. Equivalent Stress (3σ) at Circuit Pad 37

Figure 4-6. Equivalent stress (3σ) at lead frame 39

Figure 4-7. Equivalent Stress (3σ) at Solder Joint (Bottom view)............................. 41

Figure 4-8. Equivalent Stress (3σ) at Solder Joint (Isometric view)........................... 42

Figure 4-9. Selected vertex on solder joint for RPSD nodal analysis......................... 43

Figure 4-10. Response PSD in $mm2/Hz$ (Absolute to base motion)......................... 43

Figure 4-11. Response PSD in $mm2/Hz$ (Relative to base motion).......................... 44

Figure 4-12. The frequency response of normal stress at solder joint about Y axis... 46

Figure 4-13. The frequency response of directional deformation at solder joint about Y axis 47

LIST OF TABLES

Table 3-1. Approximate dimension for each part of geometry model 15

Table 3-2. Materials' mechanical properties of the parts... 18

Table 3-3. Combinations of material for each model 18

Table 3-4. Frequency breakpoints of PSD of test condition D from JEDEC Standard 22

Table 3-5. Analysis settings used for harmonic response 23

Table 3-6. Harmonic loading from PSD input 23

Table 4-1. The parameters in mesh independent study for each mesh 28

Table 4-2. The vibration mode with natural frequencies for each model 30

Table 4-3. Global directional deformation of FEA model about Y axis 32

Table 4-4. Equivalent stress at circuit pad 35

Table 4-5. Maximum equivalent stress at lead frame 38

Table 4-6. Maximum equivalent stress at solder joint 39

Table 4-7. Comparison between natural frequencies and RPSD expected frequencies 45

Table 4-8. Values of the model parameters for Steinberg's fatigue limit equation 48

Table 4-9. Number of cycles of fatigue life, N 49

Table 4-10. Miner's cumulative fatigue (CDI) values for vibration test 49

LIST OF ABBREVIATIONS

Anisotropic electrically conductive adhesive	ACA
Ball grid array	BGA
Computer-aided design	CAD
Cumulative damage index	CDI
Electrically conductive adhesive	ECA
Epoxy-terminated polyurethane	ETPU
Finite element analysis	FEA
High cycle fatigue	HCF
Isotropic electrically conductive adhesive	ICA
Low cycle fatigue	LCF
Light emitting diode	LED
Metal-oxide-semiconductor field-effect transistor	MOSFET
Plastic ball grid array	PBGA
Printed circuit board	PCB
Plastic quad flat package	PQFP
Power spectral density	PSD
Relative displacement spectral density	RDSD
Root mean square	RMS
Response power spectral density	RPSD
Sn-Ag-Cu	SAC
Surface mounted technology	SMT
Stress-life	S-N

ABSTRAK

Peranti elektronik boleh dikendalikan dalam persekitaran getaran tertentu untuk seketika tanpa mengalami kegagalan oleh sebab sambungan memainkan peranan yang sangat penting untuk melekatkan pelbagai bahagian sama sekali. Pelekat konduktif elektrik (PKE) menjadi trend bagi menggantikan pateri sebagai sambungan elektronik. Walaubagaimanapun, potensi PKE belum diterokai dengan secukupnya dalam kertas akademik. Objektif utama kajian ini adalah untuk melaksanakan penilaian kelesuan PKE akibat beban getaran. Gabungan bahan PKE yang berbeza termasuk epoksi, silikon dan akrilat diperuntukkan kepada sejumlah 8 model simulasi dengan jejaring yang berkualiti tinggi. Seterusnya, analisis modal dijalankan untuk menentukan frekuensi semula jadi dan bentuk mod model dari 0 Hz hingga 2000 Hz. Yang berikut adalah analisis getaran rawak dan analisis tindak balas harmonik dengan keluk PSD input yang dirujuk kepada Piawaian JEDEC. Akhir sekali, model kelesuan Steinberg digunakan untuk menganggar bilangan kitaran keletihan dan kerosakan akibat keletihan. Berdasarkan keputusan FEA, output maksimum tindak balas berlaku pada, frekuensi semula jadi yang mendominasi pada mod getaran pertama. Analisis ini membantu jurutera untuk mempertimbangkan untuk menukar reka bentuk untuk mengalih frekuensi semula jadi itu. Sebaliknya, peningkatan modulus keanjalan, dan kekakuan serta penurunan jisim inersia komponen boleh meningkatkan frekuensi asas yang seterusnya mengakibatkan hayat keletihan yang lanjut. Akrilat dengan modulus anjal yang tinggi dan ketumpatan jisim yang rendah dalam kalangan jenis polimer mempunyai reliabiliti getaran tertinggi untuk menahan tekanan akibat getaran berbanding PKE epoksi dan silikon. Secara keseluruhannya, kesan sifat mekanikal pateri, substrat dan bahan acuan yang berbeza dalam pemasangan papan litar terhadap relaibilti getaran pelekat konduktif elektrik (ECA) dikenal pasti.

ABSTRACT

Many devices consist of electronic parts and can be operated in a certain vibration environment for some instant without undergoing failure. Interconnection or joint plays a very important role in electronic devices to connect various electrical and mechanical parts altogether. Electrically conductive adhesives (ECA) are becoming a trend for the green substitute of solder as electronic interconnections. However, reliability of the ECA joint has not been adequately addressed in academic papers. The main objective of this study is to perform the vibration fatigue assessment of electrically conductive adhesive under vibration loading. Different combination of ECA materials including epoxy, silicone, and acrylate is assigned into a total of 8 simulation models with high-quality meshing. Next, modal analysis is carried out to determine the natural frequencies and mode shapes of model from 0 Hz to 2000 Hz. It is followed by the random vibration analysis and harmonic response analysis with the input PSD curve referred to JEDEC Standard. Lastly, Steinberg fatigue model is used to estimate the number of fatigue cycles and fatigue damage. Based on FEA results, maximum output of response occurs at, or near the dominate natural frequency at 1st vibration mode. This analysis helps engineers to consider changing the design to shift or even eliminate that natural frequency. On the other hand, it can be concluded that increasing elastic modulus, and thus stiffness as well as decreasing inertial mass of component can increase the fundamental frequency which in turn results in extended fatigue life. Acrylate with high elastic modulus and low mass density among polymer types can thus has highest vibration reliability to withstand vibration induced stress compared to epoxy and silicone ECAs. Overall, the effect of mechanical properties of different solder, substrates and die materials in a circuit board assembly on the vibration reliability of electrically conductive adhesive (ECA) is identified.

Chapter 1

INTRODUCTION

1.1 Overview of Project

According to U.S Air Force statistics, 40% of all failures observed in electronic equipment are related to connectors, 30% to interconnects, and 20% to component parts. [1] The interconnect failure is mainly due to solder degradation because solders are microstructurally unstable, and it tends to evolve with strain, temperature, and time. U.S Air Force statistics reveals that 20% of these failures are due to vibration problems. [2] While not as prevalent as thermo-mechanical solder fatigue induced by thermal cycling, vibration fatigue is also known to cause solder failures. Figure 1-1 shows the failure of ball grid array (BGA) lead-free solder joint due to vibration fatigue crack. Since then, a series of vibration test and finite element analysis (FEA) simulation were done to perform fatigue analysis and reliability testing on the solder joint.

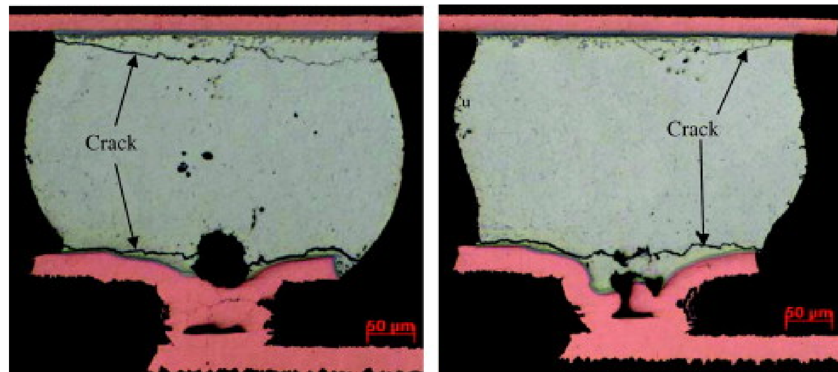

Figure 1-1. Cross sectional profile of the failed solder joints [3]

For case studies in automotive, the failure of electronic system can be attributed to high cycle fatigue due to mechanical stress induced by vibration. [4] Some common examples of random vibration include a car riding on a rough road, an airplane wing during flight and wave loads on an offshore structure. In an automobile, unbalanced rotational, reciprocating, and rolling mass causes a system destabilized, leading to random vibration. Vibration mode is the degree of freedom of vibration in a system with a specific natural frequency. The bandwidth of frequency for random vibration changes depending on its application. Steinberg explained that 2.5 tonne truck can have about 15 G and 19 G acceleration level within vibration frequencies of 15 Hz – 40 Hz

at a speed of 10 – 15 miles per hour based on test data. [5] The vibration frequency range in automobiles appears to be random from 3 Hz to 1000 Hz and increases with the chassis, suspension, and steering system. [6]

Until now, solder has been mainly used for conductive bonding of electronics components. Because of the health risks associated with toxicity of lead in lead-alloy solders, lead-free solders have gained popularity. [7] Most of the lead-free solders that have been studied thus far tend to reflow at higher temperatures than the currently utilized tin–lead solder. Also, with the recent miniaturization of electronics devices, the number of cases where resin parts or film-like materials are used is increasing. Many of these components are less resistant to heat. Therefore, as a means for conductive bonding at a low temperature, a parallel endeavour has been to investigate electrically conductive adhesives as solder substitutes due to their cheap price, easy reworking, and low processing temperatures. [8]

Adhesives have begun to develop along with the automotive electronics sector during the past ten years, where increases are anticipated in particular for the assembly and packaging of solid-state devices. Among them are light-emitting diodes (LED) used in intelligent lighting and displays in automobiles. LED lighting is apparently anticipated to rise at a rate of 10.9 percent yearly through 2013. [9] However, in order to ensure optimal performance in automotive electronic systems and to prevent subsequent quality issues, it is necessary to conduct reliability test on adhesive and have a basic understanding of their properties. This is due to the abundance of adhesives that are available as well as the variety of polymer types, forms, and formulations that are not generalized.

1.2 Problem Statement

Among the topics discussed above, there are limited literature focusing on the fatigue assessment of electrically conductive adhesive (ECA) joints under different forms of vibration. ECAs have been offered viable lead-free solder alternatives for electronic interconnections. However, the application of adhesive joints in severe vibration conditions, especially for automotive electronics is questionable whether it can minimize the fatigue failure of electronic interconnections. Therefore, the main objective of the present paper is to study the reliability and fatigue behaviour of ECAs

as the electronic interconnection under vibration loading, aiming for optimizing the adhesive performance of ECA joints in a circuit board assembly accompanied with the effect of different materials for ECAs, solder, and other electronic components such as die and substrates.

1.3 Objectives

The objectives of this project are listed as below:

1. To develop a finite element analysis (FEA) simulation to perform vibration analysis on the electrically conductive adhesive (ECA) and the test circuit board assembly.
2. To characterize reliability and fatigue behaviour of electrically conductive adhesive (ECA) joint in a circuit board assembly under vibration condition.
3. To investigate how the mechanical properties of different solder, substrates and die materials in a circuit board assembly affects the vibration reliability of electrically conductive adhesive (ECA).

1.4 Scope of Project

The study is performed through the first stage in which the CAD modelling, material assignment to the simulation model and mesh independence study are performed as pre-requisite. A FEA simulation of modal, random vibration and harmonic response analysis are later carried out to collect vibration modes, stress/deformation contour, as well as dynamic response of electrically conductive adhesive (ECA) and the components in circuit board under vibration loading with frequency range from 0 Hz to 2000 Hz. Fatigue life prediction for the electrically conductive adhesive (ECA) joint and circuit board are to be carried out using the combined method of Steinberg fatigue limit model and Palmgren-Miner's law to obtain the number of fatigue cycles and fatigue damage.

Chapter 2

LITERATURE REVIEW

2.1 Introduction

In this section, the general topics that are relatable to the research project are introduced and explained in detail with reference to journals or academic papers that are published and verified without even making involvement directly or indirectly to it. Also, common findings from the literature will be discussed.

2.2 Overview of Electrically Conductive Adhesive

H.J. Lewis et al [10] emphasized on the role and potential of electrically conductive adhesive (ECA) as solder substitute. The structure of ECAs along with their mechanical and electrical properties were explained as follows. ECAs are formulated with a binding matrix made up of most commonly used polymer such as epoxy, silicone and acrylate. It is filled with conductive material such as silver and copper. The performance of electrical conduction in ECAs are greatly affected by the microstructure of the filler material. They are further classified into isotropic (ICA) and anisotropic (ACA) based on the direction of electrical conduction. ICAs are composed of higher concentration of filler (70-80%) compared to low-cost ACAs because it conducts electricity at all direction while the conduction mechanism of ACAs is unidirectional. ICAs are by far more versatile than ACAs due to good curability. In term of electrical properties, cracking and galvanic corrosion can increase the resistance through the adhesive. Meanwhile for mechanical properties, there are many factors that affect the joint adhesion and cohesion strength of ECAs. Increasing the filler proportion will decrease the cohesion strength while switching to thermosetting polymer binder can increase adhesion strength.

In the paper of Aradhana et al work [11], the noteworthy pros and cons for ICAs are summarized and briefly discussed. ICAs take lower processing temperature than solders; they have resistance to low thermo-mechanical fatigue; they provide versatile use to ceramic and glass attachment; dispensing method like screen-printing shortened the assembly time. However, ICAs show drawbacks such as possible deterioration due to moisture, air retention and improper wetting; reworking may be required, and caution

is needed in material handling. Limitation such as low conductivity and poor impact strength comes into play when ICAs fails in high-performance application. The silver-filled epoxy ECA was also concerned in this paper. Mechanical properties and electrical properties of epoxy have strong relevance to the curing method and condition. The epoxy composite obtains increased bulk modulus for adding silver reinforcement and increased bulk resistivity for higher curing profile.

J.Y Myung et al [12] introduced the development of ECAs in the recent semiconductor packaging technologies. ICAs are used in surface mounted technology (SMT) components, die attach application, ball-grid array (BGA), flip chip package etc. For flip chip devices, ICA pastes are deposited on the substrate to supply connections between the metallic bumps and electrode in precise arrangement. Researchers are exploring the possibilities to improve the electrical conductivity of the ECAs. Among the efforts includes increase of the cure shrinkage of the polymer binder, disposal of lubricant on silver filler flake, introducing curing agent and improving the ingredients in additives. Several methods were also proposed to improve the reliability of ICA interconnects such as corrosion inhibitions, reengineering of elastic modulus, and thermal stress dissipation.

The development in enhancing ICA's impact strength were demonstrated by Daniel Lu & C.P Wong. [8] The mechanical properties of epoxy-terminated polyurethane (ETPU) were exhibited as it has good damping characteristics that substantially absorb the impact energy and enhance the impact performance of an ICA.

2.3 Fracture Behaviour of Electrically Conductive Adhesive

Aradhana et al [13] obtained the failure modes of ECAs by performing lap shear test on the epoxy and its conductive adhesives. They revealed that the adhesive failure was shifted to partially or fully cohesive failure which was caused by the interface fracture with the adherent when the shear stress increases with the shear strain.

The dependence of fracture mechanics properties of an epoxy based ECA on humidity and temperature were identified by M. Springer [14] in his paper. Figure 2-1 shows observed failure modes at the ECA joint, caused by accelerated test of thermal cycling. He concluded that the high moisture levels in the environment can reduce the resistance of the ECA interconnect to fracture, as well as catalysing debonding at less

driving forces in subcritical region compared to that in dry environments. Humidity can also change the mode of failure for an epoxy ECA. Moist environment is thereby an important criterion when assessing the failure behaviour of adhesive.

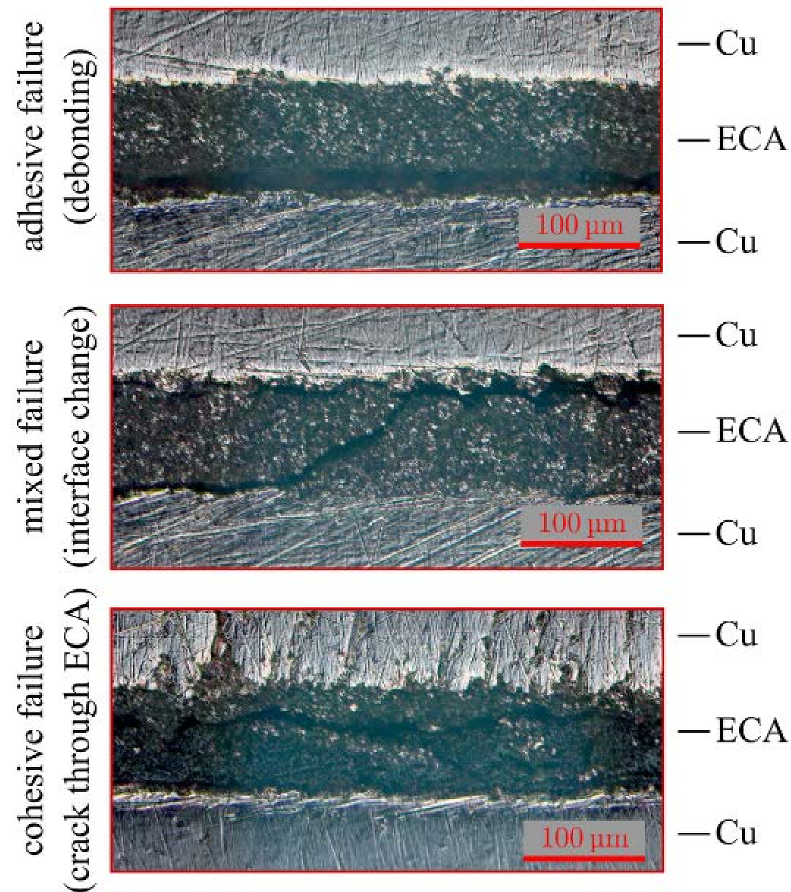

Figure 2-1. Observed failure modes at the ECA joint

Yoshiharu et al conducted an experiment [15] to investigate how the temperature affects the low-cycle fatigue (LCF) of a ICA. The results showed that when the test temperature was increased well above the glass transition point, the low cycle fatigue (LCF) life was extended, in contrast to the opposite fatigue behaviours exhibited by metals.

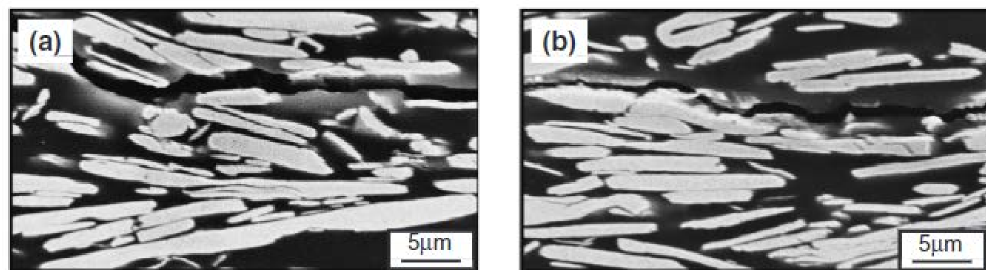

Figure 2-2. Cross sectional SEM images of fatigue tested specimens. (a) 298K (b) 398K

Figure 2-2 shows the fatigue crack propagation behaviour of the ICA specimen at the interface between silver filler and epoxy resin for different temperature. The cracks at the interface were believed to increases the electric resistance during the cycle loadings.

2.4 Random Vibration Test on Electronics Interconnection

S Zulfiqar et al [16] performed a random vibration test on LEDs that are jointed to a polycarbonate sheet by conductive adhesive. The different dispensing method for four LED models is shown in Figure 2-3 to investigate the effect to the vibration reliability of solder.

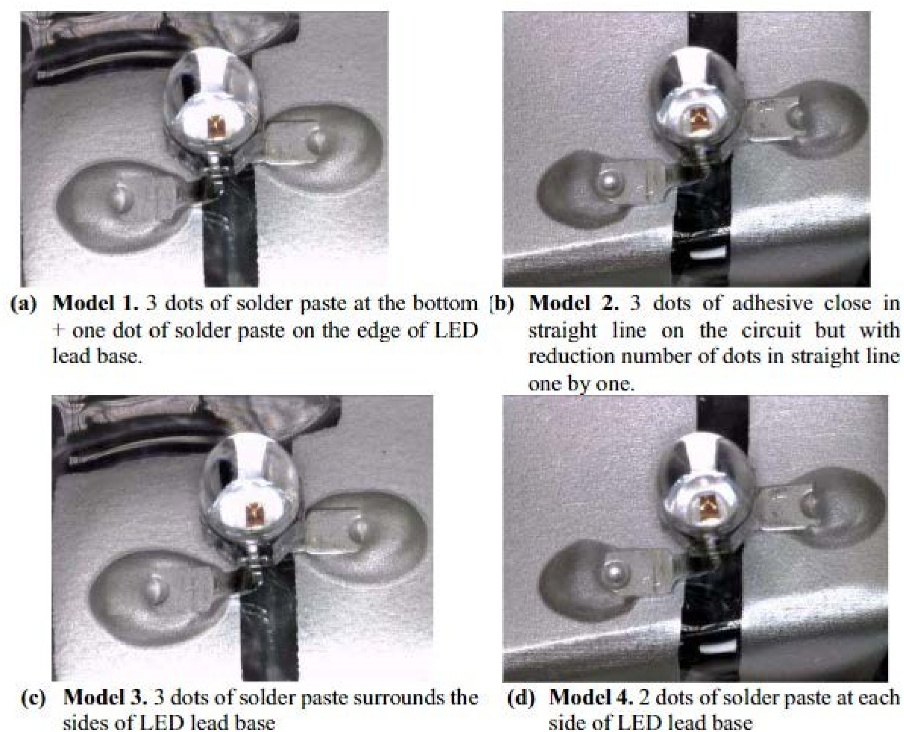

(a) **Model 1.** 3 dots of solder paste at the bottom + one dot of solder paste on the edge of LED lead base.

(b) **Model 2.** 3 dots of adhesive close in straight line on the circuit but with reduction number of dots in straight line one by one.

(c) **Model 3.** 3 dots of solder paste surrounds the sides of LED lead base

(d) **Model 4.** 2 dots of solder paste at each side of LED lead base

Figure 2-3. LED samples with solder joints

The samples were mounted on a base aluminium sheet as shown in Figure 2-4. This platform was attached on a shaker machine for swept vibration test with a frequency range from 3 Hz to 500 Hz for 4 hours. Inspection showed that that there is no debonding at either conductive adhesive or interface during vibration test. After the test, both LED and adhesive joints still remained on the circuit without cracks or voids occurrence in bonding.

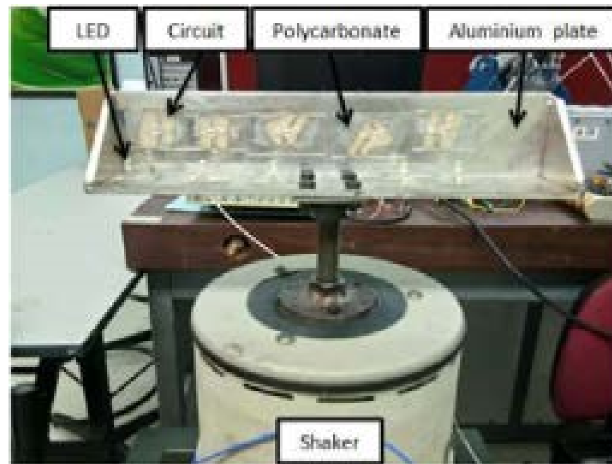

Figure 2-4. Vibration Test setup for LEDs joints

F.X. Che and John H.L. Pang [17] investigated reliability of tin alloy lead-free solder joint for the plastic quad flat package (PQFP) attached to a printed circuit board (PCB) under the random vibration test. The random vibration test setup is shown in Figure 2-5.

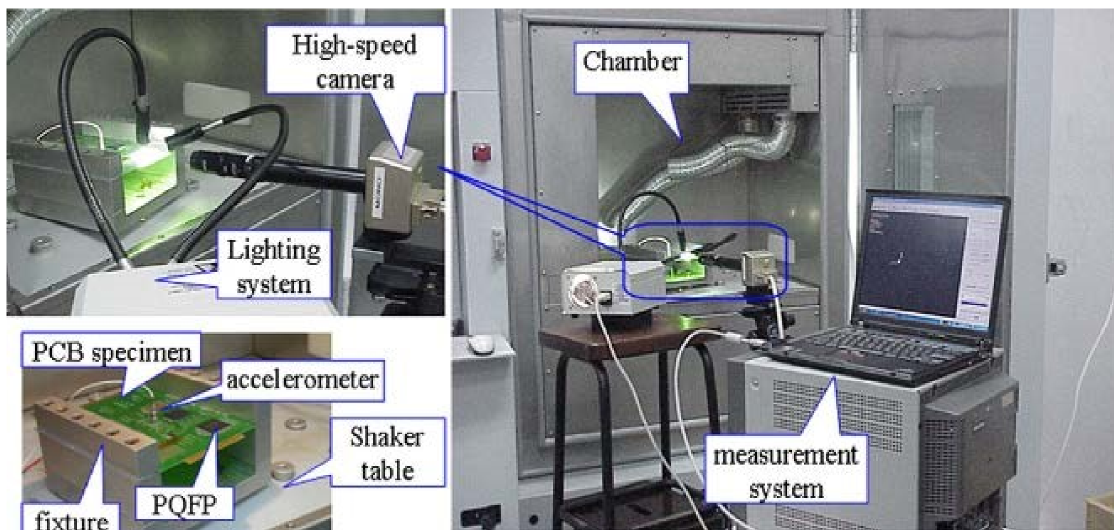

Figure 2-5. Random vibration test set up and measurement system

The PCB specimen is fixed along two edges onto the test fixture. Frequency range from 20Hz to 2000Hz was adopted for the random vibration test input profile. Specified white noise curve was used in the random vibration test with power spectral density (PSD) of 0.2 G^2/Hz. Accelerometer is used to measure the output acceleration of the PCB centre. Measurement software was used to collect dynamic response of the whole PCB free edge throughout the vibration test. The collected relative displacement

is inputted in FEA simulation to obtain solution of stress and strain for the PDFP copper lead and solder joint.

Kyeonggon Choi et al [18] demonstrated the reliability of SnCuAl(Si) solder through integrated vibration test for electronics used in automotive. The ball grid array (BGA) packages with solder balls were mounted on copper pad of a printed circuit board (PCB). Random vibration was performed in the frequency range of 400–2000 Hz by a vibrator onto a jig that connected the test samples in z-axis at the root-mean-squared acceleration of 2.5 G_{rms} until 500 thermal cycles.

2.5 Finite element analysis (FEA)

F.X. Che and John H.L. Pang [15] evaluated the stress–strain behaviour of the PQFP lead and solder joint using the displacement time history data. Figure 2-6 shows the FEA model of PCB assembly while Figure 2-7 shows the FEA model of the PQFP lead joint with boundary conditions.

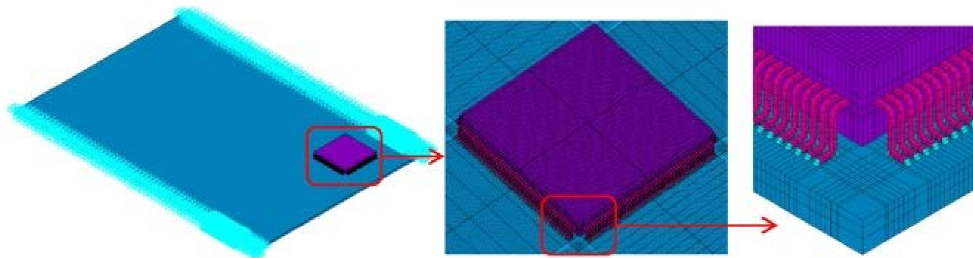

Figure 2-6. FEA model of PCB assembly for modal analysis

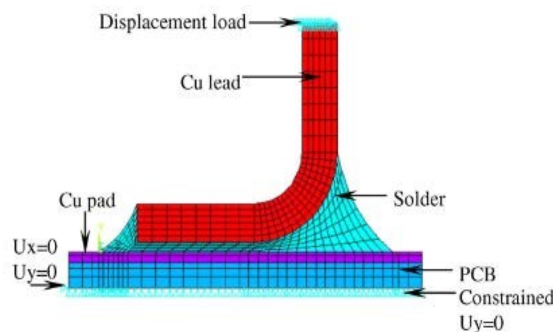

Figure 2-7. 2D FEA model and boundary condition for the PQFP lead joint

Figure 2-8 shows the von Mises stress distribution for the copper lead and solder joint. The critical stress regions were at the solder joint and copper lead.

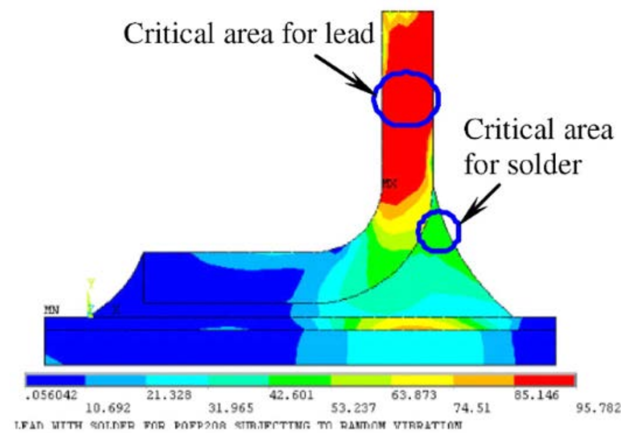

Figure 2-8. The von Mises stress contour and critical areas for Cu lead and solder joint

Y.S Chen et al [19] calculated the fatigue life of the plastic ball grid array (PBGA) under vibration loading through a series of vibration test, FEA simulation, and mathematical formulation. The displacements data in the vibration test were used in the FEA simulation.

As a result, different mesh densities are applied in the model to perform convergence study of the solution. Figure 2-9 shows that the localized conformal meshing on each single solder ball.

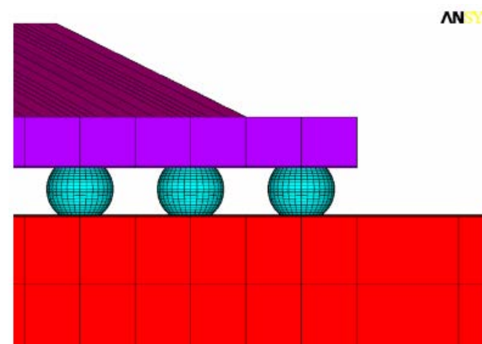

Figure 2-9. The FEA mesh of the solder balls

The responses of the PBGA component under harmonic vibration excitation were further analysed. Figure 2-10 shows the deformed shape of FEA model of PBGA, because of resonance due to harmonic loading.

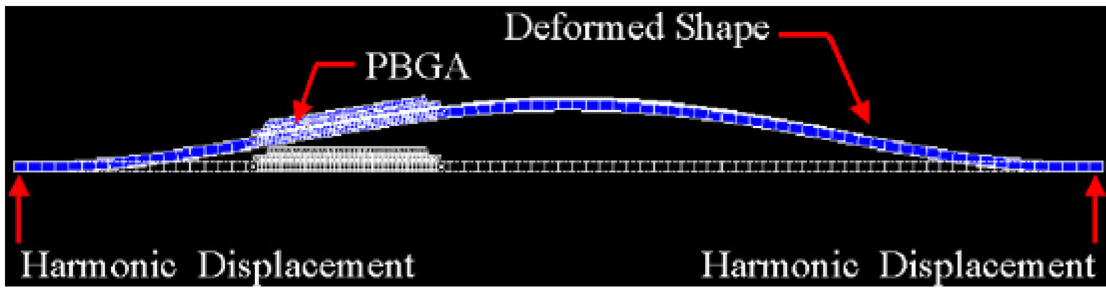

Figure 2-10. The FEA model under a harmonic vibration excitation

The local maximum stresses on each of the solder balls were inspected based on FEA result. Moreover, the corner solder ball has undergone the most stressed condition and was readily used to determine failure behaviour.

A random vibration simulation was conducted by D. Ghaderi [20] study the combined effects of vibration loading and thermal cycle on the fatigue characteristics of a solder joint in a Metal-Oxide-Semiconductor Field-Effect Transistor (MOSFET). Figure 2-11 indicated the structure and meshed geometric of FEA model.

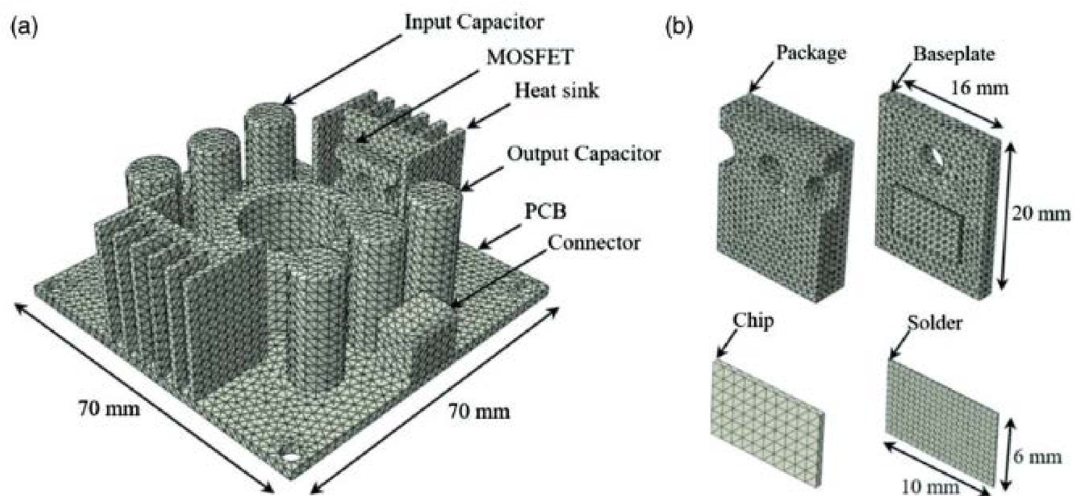

Figure 2-11. The configuration of (a) DC-DC converter and (b) MOSFET electronic package

The package was subjected to input random vibrations, and mechanical behaviour was analysed in a narrow-band frequency range that included the natural frequency. The power spectral density (PSD) function was used to normalize the input vibration. Figure 2-12 shows the frequency band range and PSD amplitudes for the study. According to the FEA findings in Figure 2-13, the corners of the solder layer experience the highest stress or strain, which diminishes as you move toward the centre.

The failure indication was the root mean square (RMS) of peeling stress. The peeling stress in the solder increases as the input vibration frequency rises.

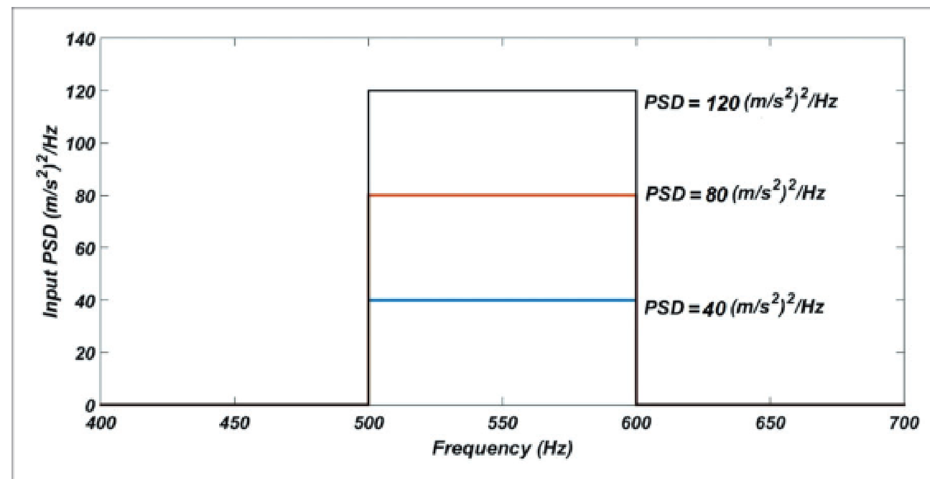

Figure 2-12. Band range of frequency and the PSD amplitudes.

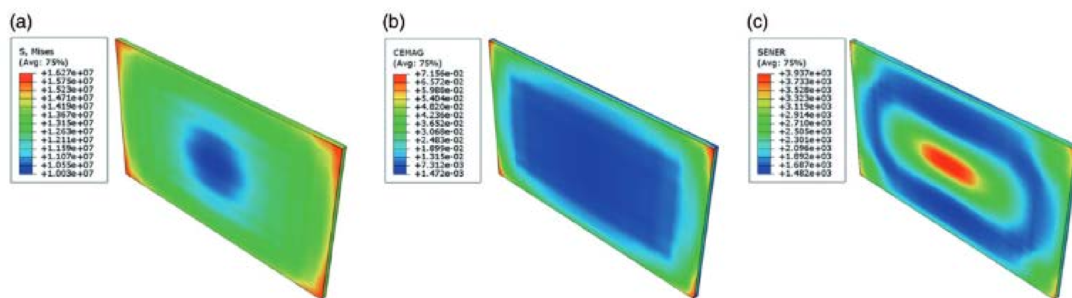

Figure 2-13. Plot of (a) stress, (b) accumulated strain, and (c) strain energy in the solder layer

2.6 Fatigue life analysis

A fatigue life predictive tool by R. Gomatam and E. Sancaktar [21] is based on experimental data for thermo-mechanical cyclic fatigue under constant maximum load and load ratio. In order to forecast changes in fatigue life based on the test variable spectrum, which also includes temperature, humidity, and load ratio, the capabilities of this predictive capacity were expanded as results. These relations allowed for the computation of the slope and intercept for the other joint within known maximum load vs number of cycles, or P-N behaviour, from which the fatigue life of the joint could be predicted. These relations were combined with knowledge of the stress states for only two joint configurations, one of which has already been characterised for the P-N behaviour. Experimental were conducted to verify the methodology's effectiveness.

A. Jouan and A.Contantinescu [22] presented a stress-life approach-based experimental fatigue investigation that was conducted on a commercial conductive silicone adhesive. The bonded assemblies underwent fatigue testing in both their virgin form and after being aged by thermo-oxidation. Based on the findings of the fatigue tests, a law was created that takes into account the effect of a thermo-oxidative ageing of the adhesive joint and relies on two mechanical predictors, including the traditional Basquin law and the threshold of dissipated energy.

With the use of the Miner's cumulative fatigue index and the Steinberg's fatigue damage calculation, Andrés García et al [23] predicted the fatigue life of the most vulnerable electronic components. The approach is based on the application of random vibration analysis to the whole instrument to determine the relative displacement, RDSD, and RMS values of the PCBs. The maximum relative displacement spectral density (RDSD) curve of the PCB is utilised as input to calculate the cumulative damage index (CDI). The benefit of this approach is that it can quickly identify the potential of fatigue damage to the electronic component based on the CDI values.

Using FEA and Steinberg's formula, Tong An et al [24] worked to model the vibration fatigue life of soldered plastic ball grid array (PBGA) assemblies. FEA was conducted to obtain the critical stress at solder joints under sine loadings. Stress life (S-N) curve of the solder joints give hints that the fatigue failure of the solder joints is in the high cycle fatigue (HCF) life scheme. Thus, the failure cycles of solder joints subjected to sinusoidal stress can be determined using Basquin's power law. In addition, a derived fatigue life prediction model is built based on the Steinberg model where it is assumed that most damage takes place in the first resonant mode The relative displacement at any PCB location can be calculated from the relation mentioned above.

2.7 Critical evaluation

These papers provide a very detailed information about the background of electrically conductive adhesives (ECAs) their recent research and development. Several studies display the fracture behaviour of ECA test sample in SEM image or strain plot under the effect of humidity and thermal cycling. Though, no literature by far shows the fracture behaviour under random vibration. Some researchers also give clear guidance on how to carry out a random vibration test using accelerated method

and FEA simulation on vibration assessment of an electronic assembly with electrically conductive adhesives (ECA) or lead-free solder. The experimental setup and frequency ranges for the vibration test in these papers are good reference to the research scope of this study. The vibration fatigue life analysis of the conductive adhesives is performed by either empirical solution, experiments alone or combining both. Notably, a validated S-N curve that shows the relationship between alternating stress and number of cycles for ECAs are hardly found to access high cycle fatigue analysis. An alternative solution is prompted to explore the new field. The method of collecting data for dynamic behaviours of vibration test samples using high-speed camera and counting cycles for strain history of the lead and solder is workable in the School with existing equipment. Yet, the presented methodology does not offer a method to study the relationship between the fatigue failure of the adhesive and the material applied. In this study, the main challenge is the determination of proper material properties for the analysis purposes. One must have careful material assignment to have a valid result corresponding to this paper's objective.

Chapter 3

RESEARCH METHODOLOGY

3.1 Introduction

In this chapter, the methodology of the study is discussed in-depth. The method to assess the vibration reliability and fatigue of the electronic interconnection using FEA simulation and computational toolbox is presented. Firstly, the development of computer-aided design (CAD) models, material selection and meshing generation are introduced. Next stage is the modal, random vibration and harmonic response analysis using FEA simulation. Lastly, the fatigue performance of the simulation model is predicted using Steinberg's approach.

3.2 FEA Geometry Modelling

A FEA geometry modelling of the digital design for LED board assembly was created in a CAD software using SolidWorks as the simulation model. It was originated from the assembly of prototype model that had been tested with experimental vibration test by previous researcher (S Zulfiqar et al) which consists of 1×LED, 1×circuit pad, 1×substrate layer and 2×solder joints. [16] It was then developed according to reference to the actual product specifications in market. The dimension for each part of geometry model is shown in Table 3-1 and Appendix A. By the way, components of the circuit pad and substrate layer was a simplified model which patterned a conventional PCB. To cater the needs for simplification of simulation, the substrate layer is laminated to the circuit pad where the LED lead is soldered to, without considering design factor for conducting circuit.

Table 3-1. Approximate dimension for each part of geometry model

Parts	Dimensions (mm)
LED	5.5×2.5×0.5
Solder joint	6.5×3.5×1.2
Circuit pad	20×15×0.08
Substrate layer	120×120×1

Notably, the rigid shape of solder joints cannot be determined easily as its final state is dependent on the reflowing condition and dispensing method. However, it is an important criterion in providing a good FEA model for simulation. The volume of

underfill, contact angle and fillet shape affects stress distribution along the solder joint under different form of loading. [25][26] S Zulfiqar et al 's solder model with optimized shape was referred as the study subject in this project. The CAD model of solder joint is shown in Figure 3-1 while the interconnections between the LED and circuit pad is shown in Figure 3-2, followed by a full view of the simulation model of LED board assembly in Figure 3-3.

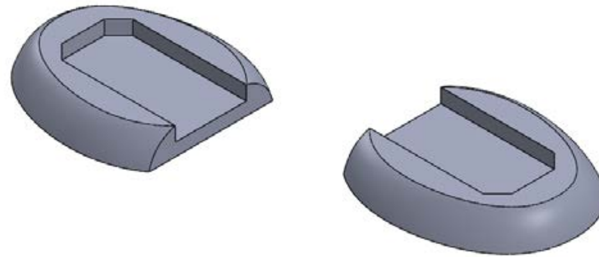

Figure 3-1. The CAD model of solder

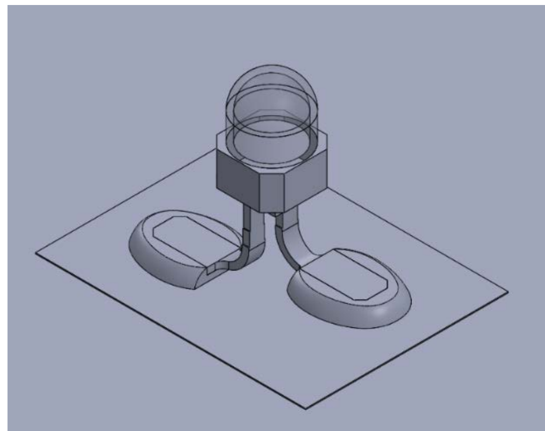

Figure 3-2. The CAD model of LED soldered on circuit pad

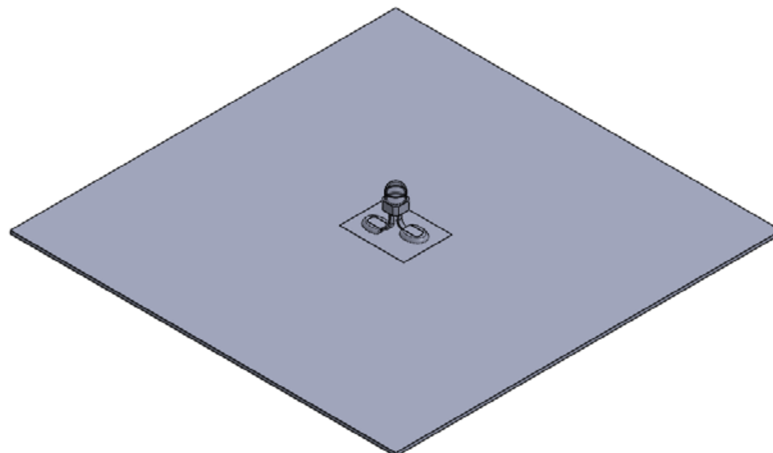

Figure 3-3. Complete assembly model

3.3 Material Assignment

Materials assignment on the part were based on several polymer types for ECAs and the common components in electronic packaging technologies as well as test model from previous researchers. Since the mechanical properties for typical materials cannot be easily determined due to a wide variety of formulations, the materials in the simulation were carefully selected to provide the simulation needs.

Epoxy adhesives were primarily chosen as study material for the solder as it is the most versatile industrial adhesives by far and it combines a lot of ideal properties for mechanical attachment. Silicone and acrylate-based alternatives were considered as their market demand is emerging to meet different application needs. [10] These adhesives are all silver-filled and in isotropic conduction for this study so that the volume fraction of filler in each type of ECAs will not differ too much and their effects induced to the mechanical properties of adhesives are nearly consistent. The same assumptions were also made to the curing method and thermo-mechanical coupling effect. This is important to improve the reliability of the simulation result. Conventional solders, which refers to traditional tin-lead solder (Sn60/Pb40) and lead-free tin alloy solder (SAC305) were also introduced in the study. [27]

For the sheet substrate, polycarbonate (PC) plastic, commonly used in PCB test fixtures were priorly chosen to carry out vibration simulation. FR-4, an industrial grade composite material composed of glass-reinforced epoxy for general-purpose PCBs and polyimide for rigid-flex circuit board applications were also included. [28] Copper metal, C10100 with high purity and optimum electrical conductivity was employed as the circuit pad material whereas copper alloy, C194 and nickel-iron alloy, Alloy 42 was assigned to the LED model as lead frame material. [29] Notably, all material was assumed to be isotropically non-linear elastic-plastic. Materials' technical data were obtained from the ANSYS material library and product specification from different manufacturers as shown in Appendix B. Materials' mechanical properties of the parts are summarized in Table 3-2.

In this study, there were 8 models based on different combinations of material for each part in the FEA assembly as shown in Table 3-3. They can be further classified into a few groups according to the material selection. The first group is among the

Model 1 to Model 5 with different solder materials that investigated how the mechanical properties of solder material affects the vibration reliability of electronic interconnections. On the other hand, the second group among Model 1, Model 6 and Model 7 with different substrate materials as well as third group among Model 1 and Model 8 with different lead frame materials investigated how those of electronic interconnections are affected by material selection for substrate layer and lead frame respectively.

Table 3-2. Materials' mechanical properties of the parts

Part	Materials	Density (kg/m^3)	Young's modulus (MPa)	Poisson ratio	Yield strength (MPa)	Ultimate tensile strength (MPa)
Circuit pad	Copper, C10100	8942	126000	0.345	250.8	210
Substrate Layer	Polycarbonate	1160	2303	0.4002	61.93	343.2
	FR-4	1900	24600	0.136	298	298
	Polyimide	1430	2760	0.34	89.6	118
Solder joint	Epoxy	3000	4600	0.3	-	-
	Silicone	4000	75	0.3	-	-
	Acrylate	1900	5900	0.3	-	-
	SAC305	7400	16600	0.3	-	-
	Sn60/Pb40	8525	29930	0.3899	34.64	57.45
Lead frame	C194	8910	121000	0.34	160	380
	Alloy 42	8120	148000	0.25	216	517

Table 3-3. Combinations of material for each model

Part	Material	Model							
		1	2	3	4	5	6	7	8
Circuit pad	C10100 Alloy	/	/	/	/	/	/	/	/
Substrate Layer	Polycarbonate	/	/	/	/	/			/
	FR-4						/		
	Polyimide							/	
Solder joint	Epoxy	/					/	/	/
	Silicone		/						
	Acrylate			/					
	SAC305				/				
	Sn60/Pb40					/			
Lead frame	C194	/	/	/	/	/	/	/	
	Alloy 42								/

3.4 Meshing

When it comes to a numerical simulation using FEA software i.e., Ansys 2022 R1, appropriate mesh densities play a critical rule to converge the solution with high accuracy, accompanied with cost efficiency and relatively low time consumption. [30] A tactical plan was executed to generate conformal mesh model where the mesh nodes between the interface of the multi-parts model is connected at a very low tolerance to facilitate effective analysis. The following approach was localized adaptive mesh refinement that was applied to regions with high potential errors such as the interconnections between solder joints and circuit pad. [31]

The meshing process was discussed in detail as follows. The very first step was set the settings to achieve meshing with high quality. The element size was remained default while the span angle centre was set to fine, followed by smoothing set to high. Then, the tetrahedron method with patch conforming algorithm that can fit more complex geometry was introduced to all bodies in the model. Next, the contact match group between connections was detected followed by setup of contact sizing in revolution type for conformal meshing. For the overall model, face sizing with hard behaviour was intuitively featured in the mesh to override global settings and get a consistent mesh of reduced size in the desired regions. There were also advanced options for Influence Volume control, which defines how the mesh is distributed along the faces for local refinement. As a result, the final mesh applied onto the models is shown in Figure 3-4 and Figure 3-5 respectively.

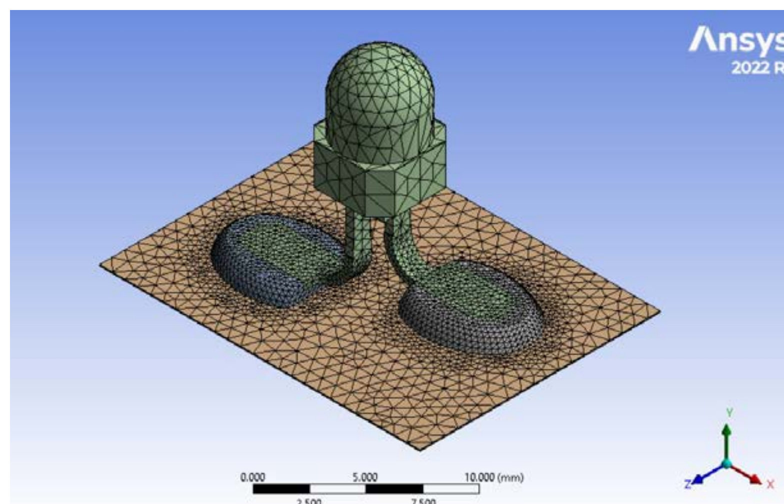

Figure 3-4. Close-up look of the mesh for LED soldered to circuit pad

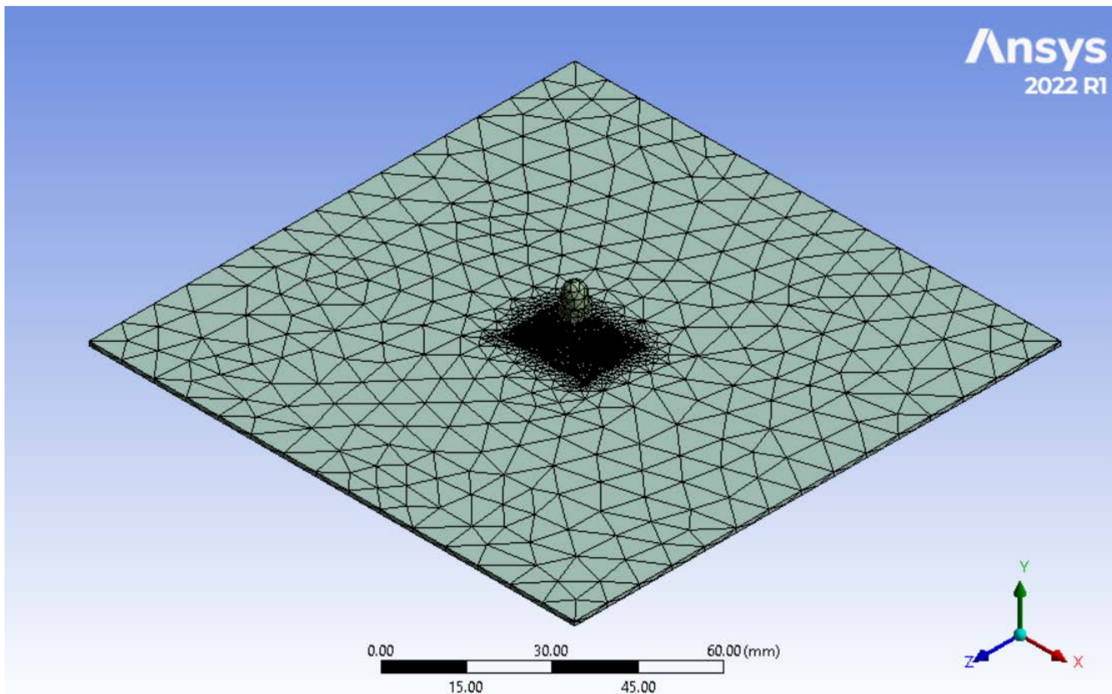

Figure 3-5. Complete mesh of the FEA simulation model

A mesh independent study was done to relate the underlying mesh to the simulation result. A few simulations that will be introduced in the following section were run with three mesh of different resolution and test evaluation was done if the simulation results changes.

3.5 Modal Analysis

As a pre-requisite for further analysis of mode-superposition method to be done, FEA models were proceeded to modal analysis to determine the vibration characteristics i.e., natural frequencies and mode shapes of linear elastic structure with response to dynamic loading. The analysis was run for all models from Model 1 to Model 8.

The setup was discussed as follows. The fixed support was located at the surface from both side of the substrate layer across the perimeter of LED component soldered to the circuit pad as shown in Figure 3-8. Next, the frequency range to find the modes is set at interval from 0 to 2000 Hz since frequencies up to 2000 Hz are interest of study for research in automotive applications. [17], [18], [32]–[34] From this analysis, the number of mode and each corresponding natural frequency between the limit range were to be identified. The mode shape and corresponding total deformation were

observed along. These modal results would be used for further dynamic analysis introduced in the following section.

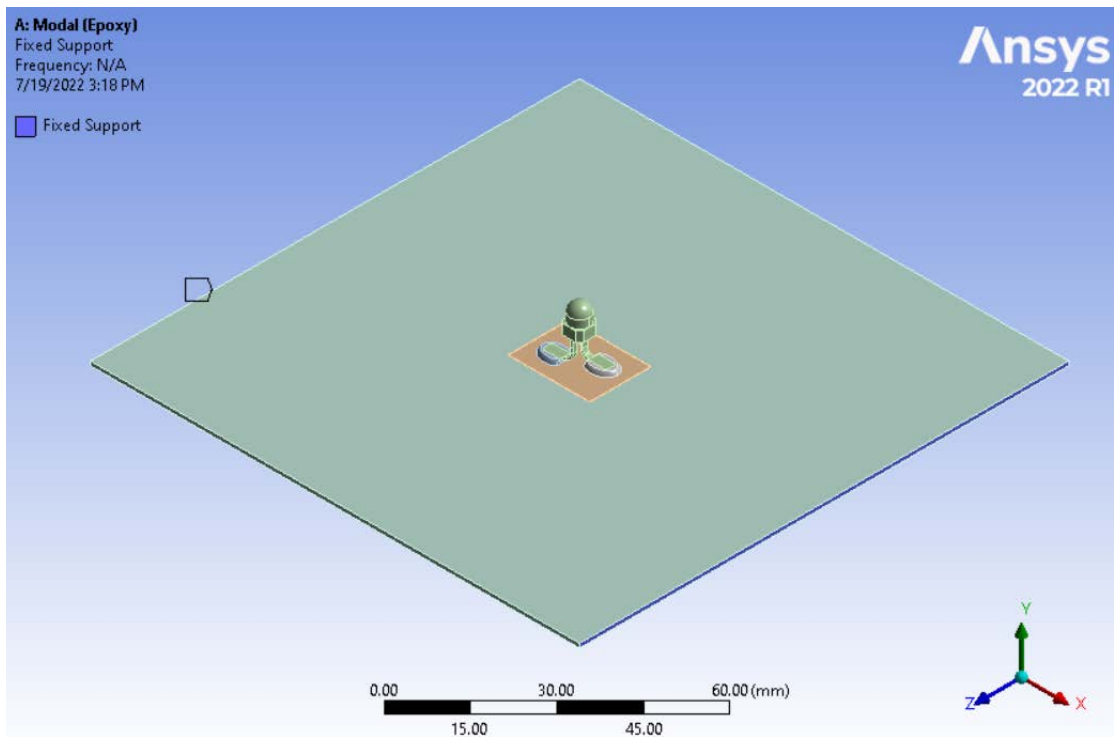

Figure 3-6. Fixed support applied on the model for modal analysis

3.6 Random Vibration Analysis

Random vibration analysis is statistical, and its randomness is characterized by the input excitation, typically called input Power Spectral Density (PSD) which are representations of vibration frequencies and energy in statistical form. It is alternative to time history where the average amplitude of excitation does not constantly change.

In this analysis, the input PSD curve was referred to the JEDEC Standard, JESD22-B103, Vibration, Variable frequency from optional stress application as shown in Appendix C. The method is to test the ability of package devices to withstand various levels of vibration because of motion produced by transportation. [35] The PSD G acceleration as input excitation selected in this analysis was based on the most severe vibration test, which is condition D where the component can be exposed to from 3 Hz to 500 Hz, as shown in Table 3-5.

The fidelity of the input PSD curve from JEDEC Standard was improved by adding an intermediate data point automatically between 70 Hz and 200 Hz and

another at 2000 Hz to meet the predetermined frequency range. Also, band limited white noise had been used to assign the PSD G acceleration value to 0.001 G^2/Hz where the spectral density has a constant value over a quantified frequency range from 200 Hz – 2000 Hz. [4] It is expected to make all the parts of the model excited at the same time. The fitted PSD input curve is shown in Figure 3-7.

Input PSD G acceleration was applied afterwards on the FEA model in Y-axis direction and perpendicular to the XZ plane. The boundary condition was remained as fixed supports selected in modal analysis. The useful results obtained from the random vibration analysis solver were reported within confidence intervals in the form of sigma values, 1σ, 2σ and 3σ, where they lie between the root-mean-squared (RMS) values over the time of occurrence, with probability of 68.3%, 95.4% and 99.73% respectively. The output solution such as directional deformation, equivalent stress, and response PSD were to be interpreted in careful manner.

Table 3-4. Frequency breakpoints of PSD of test condition D from JEDEC Standard

Frequency (Hz)	G Acceleration (G^2/Hz)
3	0.0001
6	0.003
40	0.003
50	0.013
70	0.013
200	0.001
500	0.001

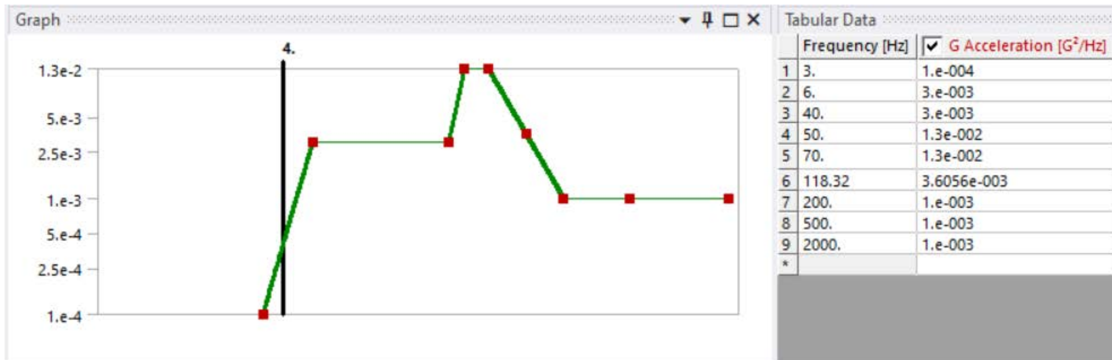

Figure 3-7. Fitted Power Spectral Density (PSD) input curve from 3 Hz to 2000 Hz

3.7 Harmonic Response Analysis

Harmonic response analysis is used to determine the dynamic response of the model structure under a steady-state sinusoidal cyclic loading at a given frequency range. The mode superposition method was used instead of full method. This method linearly combines the factored mode shape to calculate structure's response and only suitable for lightly damped systems with symmetrical matrices, which is applicable to the studied FEA model as a simplified circuit board. [36], [37]

Young's modulus, Poisson's ratio, and mass density were required as input material properties to run a harmonic response analysis. Other than that, small amount of damping was introduced in the system by setting the damping ratio to 0.02 to make the system's response more realistic. [38]

A limit search to a harmonic frequency range was set to an interval from 0 Hz – 1200 Hz in the analysis settings, which is 1.5 times narrower than modal frequency range to avoid missing contributions from modes. Then the solution interval was set at 50 intervals to get the more precise estimate. The analysis settings used for harmonic response are shown in Table 3.6. From this analysis, G acceleration of the PSD input in Table 3-4 was assigned in the simulation as the harmonic load in SI unit conversion.

Table 3-5. Analysis settings used for harmonic response

Range Minimum	0 Hz
Range Maximum	1200 Hz
Solution Intervals	50
Solution Method	Mode Superposition
Cluster Results	No

Table 3-6. Harmonic loading from PSD input

Frequency (Hz)	Acceleration (mm/s^2)
3	169.91
6	1316.1
40	3398.3
50	7909.1
70	9358.1
200	4387.2
500	6936.7
1200	10746

3.8 Vibration Fatigue Life Analysis

Steinberg's approach works in approximation of relative displacement analogue to the response measure of bending strain in classical stress-life method. The bending stress acting on the solder joints and lead frames is expected to cause the electronic assembly to undergo failure. [39]

Steinberg's fatigue model gives useful empirical formulas for calculating the fatigue limits for electronics component parts installed on circuit boards.

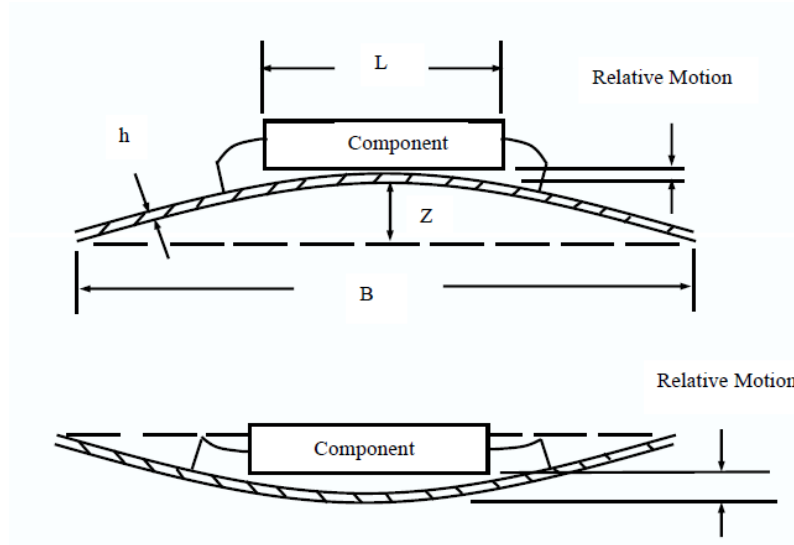

Figure 3-8. Component and Lead Wired undergoing Bending Motion

Given that Z is a displacement at the centre of the board that will give a fatigue life of around 20 million of cycle under random vibration loading in a Gaussian distribution. Steinberg's empirical formula for maximum relative displacement (3σ-RMS), $Z_{3\sigma\ limit}$ is determined by Equation 1 in unit mm.

$$Z_{3\sigma\ limit} = \frac{0.02816B}{Chr\sqrt{L}} \quad [\text{mm}] \qquad (1)$$

where

B = length of the circuit board edge parallel to the component, mm

L = length of the electronic component, mm

h = circuit board thickness, mm

r = relative position factor for the component mounted on the board (Appendix D)

C = Constant for different types of electronic component (Appendix D)